DOI: 10.48011/asba.v2i1.1050

A simple procedure for modeling and identification of a test bench 4-DOF manipulator ⋆

Davi Alexandre Paiva * **Felipe José de Sousa Vasconcelos** *
Iury de Amorim Gaspar Filgueiras *
Wilkley Bezerra Correia *

* *Department of Electrical Engineering, Federal University of Ceará, Mister Hull Ave, Fortaleza, CE, 60020-181, Brazil (e-mail: davipaiva@dee.ufc.br, felipe.sousa.vasconcelos@dee.ufc.br, iury@dee.ufc.br, wilkley@dee.ufc.br)*

Abstract: This work proposes a characterization procedure for modeling and identification of a workbench 4-DOF manipulator. The robot is a three link planar manipulator with joints connected through 4 servomotors. A decentralized approach is employed leading to four second order discrete-time linear transfer functions. Identification procedure applies amplitude modulated pseudo binary random signal (APRBS) as excitation input due to the nonlinear behavior of the system. Sensing for dynamic variables are gyroscope and accelerometers connected through an I2C protocol to a launchpad MSP432 from Texas Instruments, assembled with an ARM M4F processor. The embedded system allows sensor fusion and input signal generation such that a gray box identification may be performed. The procedure is validated through experimental data which shows the root mean square error (RMSE) with magnitude of 10^{-5} and the adjusted determination coefficient R^2_{aj} greater than 0.92 for each system. These are findings that show the effectiveness of the presented procedure herein.

Keywords: Planar manipulator, sensor fusion, embedded system, APRBS, grey box identification.

1. INTRODUCTION

Four degrees of freedom (4-DOF) robotic arm manipulators are widely used in several industrial applications due its capability of programming and handling different types of problems. Regarding its construction, lighter materials are chosen, with less filled shape, which increases its adaptability and decreases its cost. Manipulators also have higher degree of adaptability and lower price than traditional CNC machines. (Klimchik et al., 2015). The alternatives of robust control are widely used in this type of structure (Aziz and Iqbal, 2016).

Nonlinearities and coupling between links make the identification procedure of a robot manipulator a challenging task. Modeling is commonly taken from the Euler-Lagrange leading to nonlinear models (Akhtaruzzaman et al., 2009), and apply nonlinear control (Aziz and Iqbal, 2016).

On the other hand for constrained workspace and small variations in torque, one may consider the "virtual joints" approach (Klimchik et al., 2015) which leads to a linear model based on mass spring and stiffness, comprising a trade of between precision and computer resources. Such strategy may be expanded through gravity compensation (Klimchik et al., 2014), passive and active rigid identification (Alici and Shirinzadeh, 2005), MSA (Matrix Structural Analysis), FEA (Finite Element Analysis) and parametrizing methods for industrial environments (Klimchik et al., 2015).

Identification procedures are highly dependent on the choice of the input signal as the excitation of the system. From a linear perspective many methods are available such frequency response, reactive curve and the well-established least mean squares (Ljung, 1999; Aguirre, 2007). The former considers to apply a wide band input signal such as white noise or a pseudo random binary signal (PRBS). Such excitation signal is suitable for linear modeling but inadequate for nonlinear ones, for which one might consider the amplitude modulated PRBS (APRBS), as describes Nelles (2001).

Position tracking, which gives angle joints position, velocity and acceleration, may also become challenging. Specially if a choice for cheaper sensors is made. In addition, there are issues regarding to the adaptability of the robot's structure. Therefore, in order to perform the aforementioned matters as well as to fit sensors in the arm structure, this work applies gyroscope and accelerometers. These sensor units communicate through an I2C protocol with a main programming board. The I2C protocol is widely used which along with gyroscope and accelerometers is capable of sensing of the geometry and location of each link, reducing the accumulation of uncertainty along the

⋆ The authors thank DEE-UFC and CAPES for financial support to the development of this project.

robot (Klimchik et al., 2015). With the addition of a two sensor module alongside odometry, all of these elements may be combined through the kalman filter raising a sensor fusion approach which reduces uncertainties and increases the measurement accuracy (Sasiadek and Hartana, 2000).

Then, from the above discussion, this work presents a characterization procedure for modeling and identification of a test bench 4-DOF manipulator. The rest of the paper is divided as follows. Section 2 describes the manipulator workbench, section 3, presents the modeling aspects related to the identification procedure described in section 4. Section 5 exhibits the experimental results which shows the effectiveness of the identification approach, where 6 brings the conclusions.

2. MANIPULATOR BENCH DESCRIPTION

In order to evaluate the angles associated with each joint, a common DIY manipulator arm is used. The robot is assembled in the test bench showed in Fig. 1.

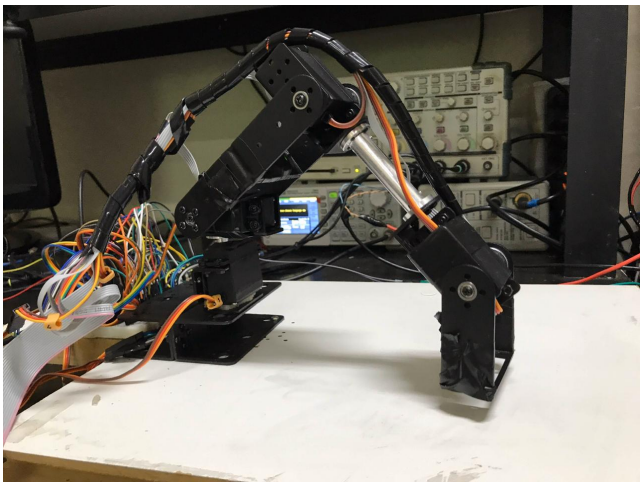

Figure 1. Test bench 4-DOF manipulator.

Design of Experiment (DoE) plays a crucial role for the robot arm model identification. The input signal might drive all of the joints and links in order to assure that the whole desired workspace is reachable.

The manipulator is constituted by links which are composed by aluminum branch legs and joints actuated by MG996R servo motors. The arm base has a revolution joint in the vertical axis with angular displacement ρ and three revolution joints in pitch angle with according to the angles θ_1, θ_2 and θ_3.

2.1 Servo motors drive

The servo motor is fed by a voltage ranged between 4,8 to 7,2 V and a PWM signal. Using the frequency of 50 Hz the duty cycle must varies between 2,5% e 12% corresponding 0° e 180°, respectively. The interface with the microcontroller is made by a circuit, shown in Figure 2, with optocouplers and a bandpass filter to avoid voltage oscillations and switching interferences.

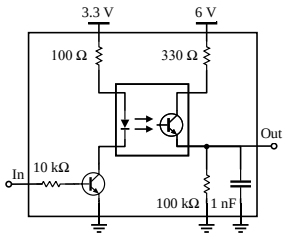

Figure 2. Servo motors drive circuit for one joint.

2.2 Measurement of signals

To measure the angles, each joint is attached to a MPU6050 module which is composed by an accelerometer and a gyroscope. This transducers send signals regarding variations on the x, y, z, xy, yz and xz axis in order to compute the angular displacement of each joint.

To obtain a more reliable measurement, it is necessary to decrease the measurement noise of the accelerometer and remove the bias from the gyroscope, that is, the multiplicative noise generated by the integration of the angular velocity. In this way, a sensory fusion is carried out between these sensors by means of a Kalman filter.

The measurement discrete system at time n is given by

$$x(n) = A_d x(n-1) + B_d u(n) + w(n) \tag{1}$$

$$y(n) = C_d x(n) + v(n) \tag{2}$$

where

$$A_d = \begin{bmatrix} 1 & -T \\ 0 & 1 \end{bmatrix}, \quad B_d = \begin{bmatrix} T \\ 0 \end{bmatrix}, \quad C_d = [1\ 0],$$

and T is the sample time.

The state vector $x(n)$ is calculated as

$$x(n) = \begin{bmatrix} \theta(n) \\ \dot{\theta}_b(n) \end{bmatrix} \tag{3}$$

where $\theta(n)$ stands to the angle measured by the accelerometer and $\dot{\theta}_b(n)$ is the gyroscope bias, which is as much that the gyroscope deflected. The true angle rate may be computed by subtracting the bias from the gyro measurement.

The input $u(n)$ is the angle rate $\theta_b(n)$ in degrees per second $(^\circ/s)$, which is given by the gyroscope measurements. The variables $w(n)$ and $v(n)$ are the process and measurement noises, respectively.

Thus, it is possible to estimate the state by design a Kalman filter calculated as

$$\hat{x}(n) = A_d \hat{x}(n-1) + B_d u(n) \tag{4}$$

$$P(n) = A_d P(n-1) A_d^T + Q_d \tag{5}$$

$$K(n) = P(n) C_d^T [C_d P(n) C_d^T + R_d]^{-1} \tag{6}$$

$$\hat{x}(n+1) = \hat{x}(n) + K(n)[y(n) - C_d \hat{x}(n)] \tag{7}$$

$$P(n+1) = [\boldsymbol{I} - K(n)C_d]P(n) \tag{8}$$

where $K(n)$ is the Kalman gain and the parameters Q_d and R_d are the process and measurement covariances, respectively.

However, due to constructive characteristics, the accelerometer is unable to provide displacement measurements made in the xy plane, because of this, to measure the ρ angle (Euler's z angle), a sensory fusion between the gyroscope and odometry is used, raised through the base servo motor identification.

2.3 Microcontroller circuit

All the signals are sent to a NXP/Freescale KL25Z Kinetis KL2 MCU microcontroller which collects the tranducers data, and actuates the drives for the servo motors and interfaces with the data acquisition system. A diagram ofthe aforementioned connections is shown in 3.

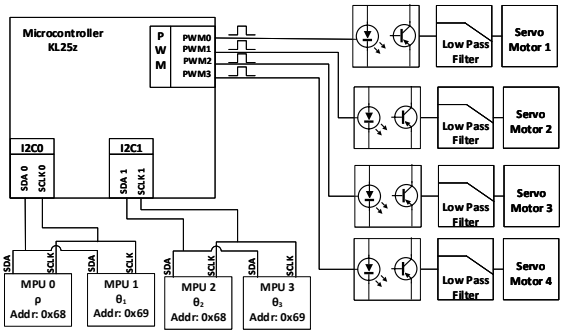

Figure 3. Diagram connection between the microcontroller servo motors and transducers circuits.

Communication between the Freescale board and position sensors (accelerometers and gyroscope) are performed through I2C protocol. In this case the microcontroller acts as the master unit whilst the sensors are slaves.

Servo motors in each joint are actuated from a driver which is controlled by a PWM input signal. So that, four PWM outputs from the Freescale board are set for such purpose. All of those PWM signals exhibit the same frequency but different duty-cycles, as the latter contains the control signal information.

3. MODELING OF THE MANIPULATOR

The modeling of a robot manipulator is an important step for the identification and control, whose model follows the rigid-body dynamics from the Newton-Euler or Lagrangian method

$$\tau = M(q)\ddot{q} + C(q,\dot{q}) + G(q) + \tau_f, \tag{9}$$

where τ_f is the friction torque, τ is the torque of the actuators, q is the position of each joint, with its correspondent velocities $\dot{q}$ and accelerations $\ddot{q}$. Parameters $M(q)$, $C(q,\dot{q})$ and $G(q)$ are the inertia, Coriolis plus centripetal and gravitational matrices, respectively, which are nonlinear terms.

However, a simplified model may be devised by the barycentric parameters or Newton-Euler parameters which lead to a linear in the paramters model (Swevers et al., 2007)

$$\tau = \Phi(q,\dot{q},\ddot{q})\gamma$$

where θ contains the barycentric parameters of each link or the barycentric of the link chains, e. g., mass or any other related properties.

Within this context, a classical approach considers the modeling based on mass, damping and stiffness parameters, leading to an equivalent second order, which can be related with equation (10) (Schappler et al., 2015; Siciliano and Khatib, 2016).

$$m\ddot{q}(t) + b\dot{q}(t) + kq(t) = f(t), \tag{10}$$

Nevertheless it delivers a simple second order model, such approach is valid only for a limited workspace area which constraints the end-effector reachable area. Thus, each link and joint of the manipulator must be modeled with its equivalent second order model. However, by considering revolute moves, displacements are joint angles $q = \theta$ and forces are torques τ, leading to the model

$$m\ddot{q}(t) + b\dot{q}(t) + kq(t) = \tau(t), \tag{11}$$

Modeling from Eq. (11) regards similarities with that in Eq. (9), although it comprises a much simpler one. Such similarities come from considering the mass m of the link chain instead of $M(q)$, while τ_f turns into $b\dot{q}(t)$ and $G(q)$ is partially incorporated by $kq(t)$, whereas $C(q,\dot{q})$ finds no counterpart and then, is neglected. Obviously so many simplifications result in a model mismatch.

By considering such simple model which is linear in the parameters it becomes easier to perform any well-established identification method, such as least-squares. Moreover, it also allows one to consider a simpler feedback control design. Nevertheless, such simplification may require any sort of additional control branches in order to counteract all of the neglected terms and variables.

So that, the aforementioned considerations make the identification method herein suitable for robot manipulators with small dimensions and masses. In addition, a light and workbench manipulator for educational purposes may benefit from the identification procedure herein as it lead to an equivalent well known mass-spring-damper system model.

All the parameter estimation of the system is made by software, therefore the continuous-time model from (10) must be discretized in difference equations in order to allow numerical calculations. This work takes the forward Euler discretization, following equation (12).

$$\frac{dq(t)}{dt} \approx \frac{q[nT] - q[(n-1)T]}{T}. \tag{12}$$

So, the discrete-time representation of the joint systems is given by

$$q(n) = \frac{1}{1 + \frac{kT^2}{m} + \frac{bT}{m}} \left[\left(\frac{bT}{m} + 2 \right) q(n-1) - q(n-2) + \frac{\sigma T^2}{m} u(n) \right] \quad (13)$$

where $n = 1, 2, \ldots, N$ with N is the number of data samples and T is the sample time interval.

4. MODEL IDENTIFICATION PROCEDURE

As any identification procedure, a model structure is previously defined, so parameters of it may be identified from an input-output relationship. In a case where the system is a robot arm as herein, previous section has discussed about an equivalent mass-spring-damper as a proper model to describe the plant within a defined workspace.

So that, by taking such a model, one seek for an equivalent second order input-output relationship, whose general discrete-time equation is set as

$$G(z^{-1}) = \frac{Kz^{-1}}{1 + a_1 z^{-1} + a_2 z^{-2}}. \quad (14)$$

Therefore, identification procedure is about obtaining parameters K, a_1 and a_2 in equation (14) which best describe the behavior of the plant.

For such purpose, the wider the band one excites the plant the more accurate the model is (Aguirre, 2007). Then, it turns mandatory to constraint the workspace of the bench robot arm within proper boundaries for which an input-output relationship as the one in equation (14) is valid. So that a pseudo random signal able to lead the robot arm to be driven inside the desired workspace may be devised, as normally done for any system (Ljung, 1999). Within this context, this section is splitted in two subsections where one of those describe the analog pseudo random binary signal (APRBS) followed by a structure model parameter estimation section.

4.1 Input APRBS signal generation

The proper choice of the excitation signal is probably the most important aspect regarding to the DoE, specially if it is intended to be applied for a nonlinear plant. So that, it is a challenging issue to assure that the input signal comprises both a wide band of frequencies and lead the system to capture essential output information.

The well known pseudo binary random signal (PRBS) is one of the most commonly considered input signals for the most of the DoE for linear system identification. It does lead to an accurate linear model if the transfer function parameters regard a linear relationship with the observed dynamics. This type of input signal makes the input of the system to randomly vary between two different levels, with holding time T_h for each level.

In a case of a nonlinear system that exhibits weak interaction between nonlinear terms the application of a PRBS signal may be enough as it makes the system to vary within a small range of operation. In a wider range of operation, switching the input signal between two different levels may not be enough to get all the information needed from the output, even for small nonlinear interaction. For such cases one may consider to apply a multilevel signal limited to a minimum u_{min} and a maximum u_{max}, producing the so called amplitude modulated pseudo binary random signal (APRBS), as described in (Deflorian and Zaglauer, 2011; Nelles, 2001)

The set of chosen input signals herein is a typical APRBS signal as described in Eq. (15).

$$\mathcal{U} = \sum_{s=0}^{N} u_s(d_s, T_h) \quad (15)$$

where $d_s \in [u_{min}, u_{max}]$ is the modulated amplitude which remains applied to the plant during T_h dwell time (Deflorian and Zaglauer, 2011). The number of levels N for u_s are randomly chosen following the procedure described in (Nelles, 2001, p.p. 570)

4.2 Embedded system description

Data is acquired by serial communication between the microcontroller board and the desktop computer. Time sample is $T = 10\ ms$ when angles (plant output) and reference signal are all updated. Data is stored in order to have separate files, one for identification purposes and another one for validation, which primarily specifies the test duration.

Identification setup depends on the desired workspace for the robot manipulator as its constraints ultimately give maximum and minimum limits for the each angle of each joint. Test is performed separately for each link while all the other links remain still with its motors keeping them in a fixed position. The angles of the links in each joints that are not under test are chosen such as the arm configuration matches the one it will perform in the workspace.

For the basis, joint angle is chosen to vary in the range -1.26 rad $< \rho <$ 1.20 rad. For link 1 0.562 rad $< \theta_1 <$ 1.972 rad, for link 2 0.9617 rad $< \theta_2 <$ 3.142 rad and for link 3 0.5108 rad $< \theta_3 <$ 4.5 rad. These limits are graphically represented in Fig. 4.

4.3 Structure model

In order to reduce the effort of the parameter estimation algorithm, average level for input and output signals of each joint are removed, leading one to get the estimation signal to be as

$$q_f = q_m - \frac{1}{N} \sum_{i=1}^{N} q_{m_i} \quad (16)$$

where q_f and q_m are the filtered and measured signals, respectively for either input or output.

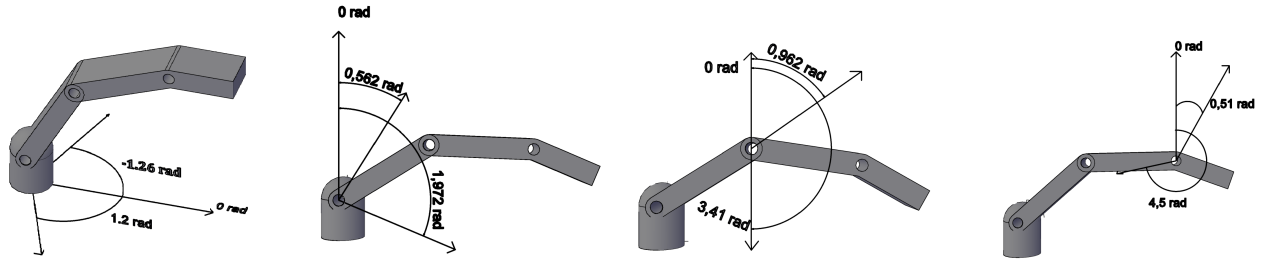

(a) (b) (c) (d)

Figure 4. Manipulator angles for (a) joint 1, (b) joint 2, (c) joint 3 and (d) joint 4.

Based on the discrete-time model from equation (13) it is possible to determine a predictor for formulating the parameter estimation problem (Ljung, 1999). However, to achieve this purpose the discrete-time model must be rewritten as

$$\hat{q}(n|\theta_i) = \varphi^T(n)\theta_i. \tag{17}$$

Taking into account the experimental data $Z_i^{N_E}$ collected for the estimation, one can define a cost function expressed by

$$V(\theta_i, Z_i^{N_E}) = \frac{1}{N_E}\sum_{n=1}^{N_E}\left[q_i(n) - \hat{q}(n|\theta_i)\right]^2 \tag{18}$$

where N_E represents the number of data points selected in the parameter estimation, $n = 1, 2, \ldots, N_E$, i stands for the number of joints, y_i is the measured angle and $\hat{y}_i$ is the estimated angle for each joint. Finally, the parameter estimate for each joint is found with a numerical algorithm designed to solve (Ljung, 1999)

$$\hat{\theta}_i = \underset{\theta_i}{\operatorname{argmin}}\, V(\theta_i, Z_i^{N_E}). \tag{19}$$

Model validation It is important to determine the quality of the estimated model and for this the experimental Z^{N_V} data of validation collected are used. The criteria chose to compute the accuracy of the model is the root mean square error (RMSE) given by

$$\Omega(\hat{\theta}_i, Z_i^{N_V}) = \sqrt{\frac{1}{N_V}\sum_{n=1}^{N_V}\left[q_i(n) - \hat{q}(n|\theta_i)\right]^2} \tag{20}$$

and the adjusted determination coefficient R^2_{aj}, which should fit $0 \leq R^2_{aj} \leq 1$ where values close to 1 represent a better adjusted model. It can be computed as

$$R^2_{aj}(\hat{\theta}_i, Z_i^{N_V}) = 1 - \left(\frac{N_V - p}{N_V - 1}\right)\frac{\sum_{n=1}^{N_V}\left[q_i(n) - \hat{q}(n|\theta_i)\right]^2}{\sum_{n=1}^{N_V}\left[q_i(n) - \bar{q}(n|\theta_i)\right]^2} \tag{21}$$

where $N_V = N - N_E$ and p is the number of parameters of the model.

Gray box identification algorithm Whereas that the mass parameter m can be more easily measured using precision scales, this feature may be incorporated into the identification algorithm. A suitable way to accomplish this can be promoted as described in Algorithm 1.

Algorithm 1 Pseudocode for joints identification

```
T ← sample time
m ← mass of the joint
Initialize σ, b and k
procedure ESTIMATION
    for i = 1 → N_E do
        Calculate φ(n)
        Calculate θ(n) using the chosen estimation algorithm incorporating the coefficients of the equation (13)
        Update the parameters σ, b and k based on θ(n) and the coefficients of the equation (13)
    end for
    for i = 1 → N_E do
        Calculate the estimated q̂_E(n) using equation (13)
    end for
    Calculate the residue Σ_{n=1}^{N_E}((q_i − q̂_{V_i})^2)
    Calculate V(θ_i, Z_i^{N_E})
end procedure
procedure VALIDATION
    for i = 1 → N_V do
        Calculate the estimated q̂_V(n) using equation (13)
    end for
    Calculate Ω(θ̂_i, Z_i^{N_V})
    Calculate R^2_{aj}(θ̂_i, Z_i^{N_V})
end procedure
```

5. RESULTS

The experimental data, as mentioned before, was split into two parts for each joint. The first eighty percent of data were used for parameter estimation, whilst the other twenty percent were used for model validation.

In order to estimate the discrete-time models parameters, the extended recursive least squares (ERLS) algorithm (Astrom and Wittenmark, 1994; Chen, 2004) was used. Thus, the models are considered as stochastic systems, which means that each differential equation is rewritten as a autoregressive-moving average with exogenous terms (ARMAX) process (Ljung, 1999), expressed by

$$A(z)y(n) = B(z)u(n) + C(z)e(n), \tag{22}$$

where $y(n)$, $u(n)$ and $e(n)$ are the model output, input and the system noise, respectively.

Considering that it is not possible to know the noise *a priori*, the ARMAX model has the drawback that it is not possible to convert it directly into a regression model. In order to overcome this problem, the noise is approximated by the residual vector, according to equation (23)

$$\varepsilon(n) = q(n) - \varphi^T(n)\hat{\theta}(n), \tag{23}$$

where the parameter vector is given by

$$\theta = [a_1 \ ... \ a_{n_a} \ b_1 \ ... \ b_{n_b} \ c_1 \ ... \ c_{n_c}]^T \tag{24}$$

and the regression vector is

$$\varphi^T(n) = [-y(n-1) \ ... \ -y(n \ - \ N) \ u(n-1) \ ... \ u(n-N) \ \varepsilon(n-1) \ ... \ \varepsilon(n-N)]. \tag{25}$$

For the discrete-time model of the manipulator the parameters vectors were defined with $T = 0.01$ seconds in the ARMAX structure and computed as

$$\theta_i(n) = \frac{1}{1 + \frac{k_i(n)T^2}{m_i} + \frac{b_i(n)T}{m_i}} \left[\left(-\frac{b_i(n)T}{m_i} - 2\right) \quad 1 \quad \frac{\sigma_i(n)T^2}{m_i} \quad c_i\right]^T \tag{26}$$

where i indicates the number of joint.

The parameters update in Algorithm 1 with the measured mass m incorporated can be calculated as

$$b_i(n+1) = \frac{(1 - \theta_i[2](n))\theta_i[1](n) + (\theta_i[1](n) + 2)\theta_i[2](n)}{(\theta_i[1](n)T - q_i(n))\theta_i[2](n)}, \tag{27}$$

$$k_i(n+1) = -\frac{m_i}{\theta_i[1](n)T^2}(\theta[1](n) + 2 + b_i(n)q_i(n)) \tag{28}$$

and

$$\sigma_i(n+1) = \frac{m_i\theta_i[3](n)}{T^2}\left(\frac{1 + k_i(n)T^2}{m_i} + \frac{b_i(n)T}{m_i}\right). \tag{29}$$

After the parameter estimation step, the cost functions $V(\hat{\theta})_i$ were calculated, followed by the validation step. Finally, the performances criteria $\Omega(\hat{\theta}_i)$ and $R^2_{aj}(\hat{\theta}_i)$ were computed. The results are presented in Table 1.

The models determined by the parameters calculated are suitable considering that they present small values for $V(\hat{\theta})_i$ and $\Omega(\hat{\theta}_i)$ as well as produce values of $R^2_{aj}(\hat{\theta}_i)$ close to 1.

The comparison between the measured and the identified models signals, that is, both the estimation and validation data are shown in Figure 5.

Table 1. Manipulator parameters and performances criteria for mass-sprig models

	Joints			
Parameter estimated	1	2	3	4
m (kg)	0.294	0.239	0.144	0.072
b (Nm/(rad/s))	19.1138	2.4919	6.5824	2.3477
k (Nm/rad)	1778.9	114.0636	113.2759	41.9973
σ (N/rad)	1801.6	106.5490	118.6264	33.7255
Performance criteria				
$V(\hat{\theta})$	0.0086	0.0175	0.0146	0.0052
$\Omega(\hat{\theta})$	1.35×10^{-5}	3.68×10^{-5}	4.68×10^{-5}	2.12×10^{-5}
$R^2_{aj}(\hat{\theta})$	0.9970	0.9263	0.9863	0.9931

6. CONCLUSIONS

This work has shown a grey box identification procedure for a three link planar manipulator. The nonlinear nature of the plant led to the APRBS as input excitation signal. Measurements of position, velocity and acceleration are performed through sensor fusion leading to accurate values. Results show that the second order model based on barycentric approach is suitable to properly describe the behavior of the planar arm for constrained workspace, though. However, the second order model allows one to consider it for the design of the linear feedback control, which is part of a robot arm controller.

ACKNOWLEDGMENT

The authors thank to DEE-UFC and CAPES for financial support to the development of this project.

REFERENCES

Aguirre, L.A. (2007). Introdução à identificação de sistemas. *3ª Edição, Ed. UFMG, Minas Gerais, Brazil, 730p.*

Akhtaruzzaman, M., Akmeliawati, R., and Yee, T.W. (2009). Modeling and control of a multi degree of freedom flexible joint manipulator. In *2009 Second International Conference on Computer and Electrical Engineering*, volume 1, 249–254. IEEE.

Alici, G. and Shirinzadeh, B. (2005). Enhanced stiffness modeling, identification and characterization for robot manipulators. *IEEE Transactions on Robotics*, 21(4), 554–564. doi:10.1109/TRO.2004.842347.

Astrom, K.J. and Wittenmark, B. (1994). *Adaptive Control*. Addison-Wesley Longman Publishing Co., Inc., USA, 2nd edition.

Aziz, H.M.W. and Iqbal, J. (2016). Flexible joint robotic manipulator: Modeling and design of robust control law. In *2016 2nd International Conference on Robotics and Artificial Intelligence (ICRAI)*, 63–68. IEEE.

Chen, H. (2004). Extended recursive least squares algorithm for nonlinear stochastic systems. In *Proceedings of the 2004 American Control Conference*, volume 5, 4758–4763. IEEE.

Deflorian, M. and Zaglauer, S. (2011). Design of experiments for nonlinear dynamic system identification. *IFAC Proceedings Volumes*, 44(1), 13179 – 13184. doi: https://doi.org/10.3182/20110828-6-IT-1002.01502.

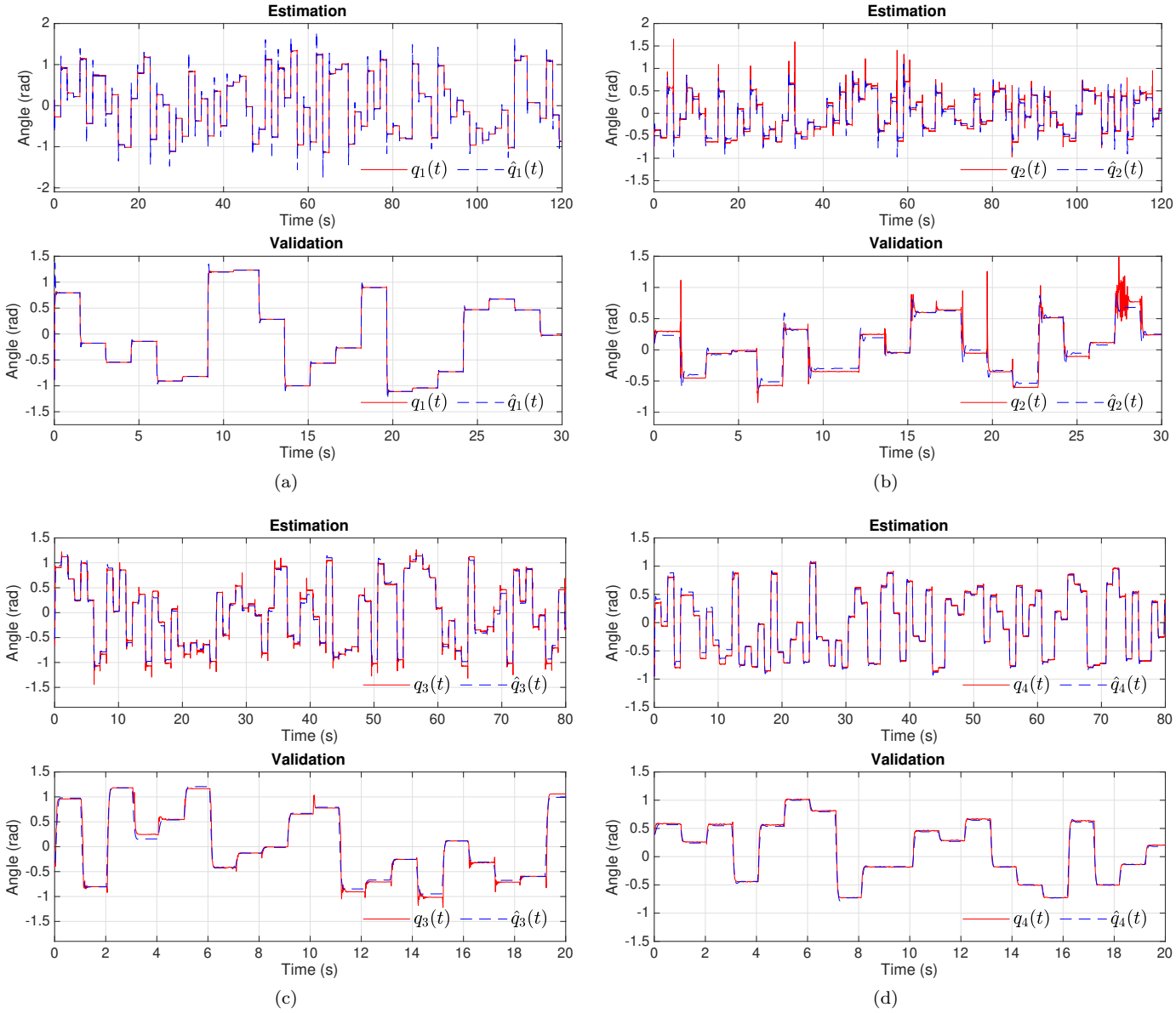

Figure 5. Angles curves from (a) joint 1, (b) joint 2, (c) joint 3 and (d) joint 4, considering the measured signal and the identified model response for both estimation and validation.

URL `http://www.sciencedirect.com/science/article/pii/S1474667016457381`. 18th IFAC World Congress.

Klimchik, A., Caro, S., Wu, Y., Chablat, D., Furet, B., and Pashkevich, A. (2014). Stiffness modeling of robotic manipulator with gravity compensator. In *Computational Kinematics*, 185–192. Springer.

Klimchik, A., Furet, B., Caro, S., and Pashkevich, A. (2015). Identification of the manipulator stiffness model parameters in industrial environment. *Mechanism and Machine Theory*, 90, 1 – 22. doi:https://doi.org/10.1016/j.mechmachtheory.2015.03.002.

Ljung, L. (1999). *System Identification (2nd Ed.): Theory for the User*. Prentice Hall PTR, USA.

Nelles, O. (2001). *Nonlinear system identification. From classical approaches to neural networks and fuzzy models*. doi:10.1007/978-3-662-04323-3.

Sasiadek, J. and Hartana, P. (2000). Sensor data fusion using kalman filter. In *Proceedings of the Third International Conference on Information Fusion*, volume 2, WED5–19. IEEE.

Schappler, M., Vorndamme, J., Todtheide, A., Conner, D.C., von Stryk, O., and Haddadin, S. (2015). Modeling, identification and joint impedance control of the atlas arms. In *2015 IEEE-RAS 15th International Conference on Humanoid Robots (Humanoids)*, 1052–1059. IEEE.

Siciliano, B. and Khatib, O. (2016). *Springer handbook of robotics*. Springer.

Swevers, J., Verdonck, W., and De Schutter, J. (2007). Dynamic model identification for industrial robots. *IEEE Control Systems Magazine*, 27(5), 58–71.